

A Differential Abundance Analysis of HD219175 A and B*

Hua-Wei Zhang¹ and Gang Zhao²

¹ Department of Astronomy, School of Physics, Peking University, Beijing 100871;
zhw@bac.pku.edu.cn

² National Astronomical Observatories, Chinese Academy of Sciences, Beijing 100012

Received 2004 November 11; accepted 2005 March 3

Abstract The abundances of the wide binary pair HD 219175 A and B are determined and compared using a line-by-line differential analysis. No evidence for difference has been found in the abundances of Fe, O, Na, Mg, Al, Si, K, Ca, Sc, Ti, V, Cr, Mn, Ni, Cu and Ba. Our results support a physical relation between the two components of HD 219175.

Key words: stars: abundances — stars: atmospheres — binaries: visual

1 INTRODUCTION

The formation and evolution of binary stars is an interesting subject in stellar evolution and is still mostly a puzzle. In recent years, some authors have begun to study the abundance difference between the components of binary systems.

Laws & Gonzalez (2001) found that 16 Cyg B is slightly more metal-rich than 16 Cyg A. Gratton et al. (2001) performed a differential analysis for six visual main sequence binaries. They found between HD 219542 A and B there is a 0.09 dex difference in their iron content. Sadakane et al. (2003) also found the abundances of Fe, Sc, and Ti are definitely higher (by 0.05 dex) in component A of HD 219542 than in component B while no evidence of any differences in other elements. Desidera et al. (2004) presented an analysis of iron abundances for 23 wide binaries, but they did not find significant abundance difference in HD 219542 A and B.

If the abundance differences found in components of binary systems are real, how did these differences come about since these components presumably share a common primordial environment? To answer this question, much more accurate abundance investigations are needed.

The V magnitudes of HD 219175 A (HIP114702) and B (HIP114703) are 7.57 and 8.19, and their spectral types are F9V and G3V, respectively. The Hipparcos Survey (ESA, 1997) showed they are possible optical double stars, while Tokovinin & Smekhov (2002) argued that they are wide resolved visual binaries. In this paper, we present the results of a differential abundance analysis for HD 219175 A and B.

* Supported by the National Natural Science Foundation of China.

2 OBSERVATIONS AND DATA REDUCTIONS

Spectroscopic observations of HD219175 A and B were carried out with the Coudé Echelle Spectrograph attached to the 2.16m telescope at the National Astronomical Observatories (Xinglong, China) on 2003 November 12. The red arm of the spectrograph with a 31.6 grooves/mm grating was used in combination with a prism as the cross-disperser, providing a good separation for the different echelle orders. With a 0.5mm slit ($\sim 1.06''$), the resolving power was 37000 in the middle focus camera system. The detector was a Tek CCD (1024×1024 pixels with $24 \times 24 \mu\text{m}^2$ each in size). The signal-to-noise ratio of the spectra at 6400 Å is about 150 pixel^{-1} . The wavelength coverage is from 5700 Å to 8800 Å with some gaps. A detailed description of the technical aspects of the spectrograph can be found in Zhao & Li (2001).

A reduction of two-dimensional echelle spectral data was performed using the ESO MIDAS software package. The data reduction includes locating the echelle order on the multi-order two dimensional spectrum; subtracting the background; and extracting the orders by summation along the slit. The pixel-to-pixel variation was corrected by dividing flat-field taken at the same night. The wavelength calibration was based on a thorium-argon lamp. Spectra of bright, rapidly rotating, spectral type B stars observed during the observational run were used to divide out the telluric O₂ features. The radial velocities were measured from about 20 intermediate strong and unblended lines and results for HD 219175A and B are -31.14 and -22.58 km s^{-1} , respectively, with an accuracy of 1.5 km s^{-1} .

The spectra were then normalized by a continuum function determined by fitting a spline curve to a set of pre-selected continuum windows (typically 20–30 per order) taken from the solar atlas.

The equivalent widths (*EWs*) were measured by direct integration or Gaussian fitting, depending on which method gave the best fit of the line profile. Usually, weak lines are well fitted by a Gaussian profile. If unblended lines are well separated from nearby lines, direct integration is the best method. The list of lines is the same as used in Zhang & Zhao (2004). Finally, *EWs* of 76 lines of Fe I, Fe II, Li I, O I, Na I, Mg I, Al I, Si I, K I, Ca I, Sc II, Ti I, V I, Cr I, Mn I, Ni I, Cu I and Ba II were obtained. The error of the *EW* measurement is 2–3 mÅ.

3 ABUNDANCE ANALYSIS

The effective temperature was determined from $b - y$ and $V - K$ colour indices using the IRFM calibrations of Alonso et al. (1996). The surface gravity was calculated using the method described in Chen et al. (2000). Hipparcos parallaxes (ESA, 1997) of HD 219175 A and B are 26.52 ± 2.41 , $35.69 \pm 5.65 \text{ mas}$, respectively. Nordström et al. (2004) gave a photometric distance of 37 pc for HD 219175 B which is quite consistent with the 38 pc Hipparcos parallax for HD 219175 A. This implies the error of Hipparcos parallax for HD 219175 B is larger than Hipparcos survey claimed. So, the photometric distance was adopted for surface gravity calculations of HD 219175 B. With the effective temperature and absolute magnitude, the stellar mass was determined from the star's position in the $M_V - \log T_{\text{eff}}$ diagram by interpolating the evolutionary tracks of VandenBerg et al. (2000). The microturbulence (ξ_t), was obtained by requiring a zero slope of $[\text{Fe}/\text{H}]$ vs. *EW*. The whole procedure of deriving T_{eff} , $\log g$ and ξ_t was iterated until convergence, when the spectroscopic $[\text{Fe}/\text{H}]$ value was obtained. Uncertainties in the parameters, $\pm 70 \text{ K}$ in T_{eff} , ± 0.10 in $\log g$, $\pm 0.2 \text{ km s}^{-1}$ in ξ_t , and ± 0.05 in $[\text{Fe}/\text{H}]$ are expected. Table 1 lists the atmosphere parameters of HD 219175 A and B along with their masses.

In Fig. 1 we show the abundance differences obtained from Fe I and Fe II lines plotted against the excitation potential of lower energy level (LEP) and the mean *EW* value of the two

components ($\langle EW \rangle$). We can see that there is no obvious trend in these two plots. It implies that stellar parameters we used are accurate.

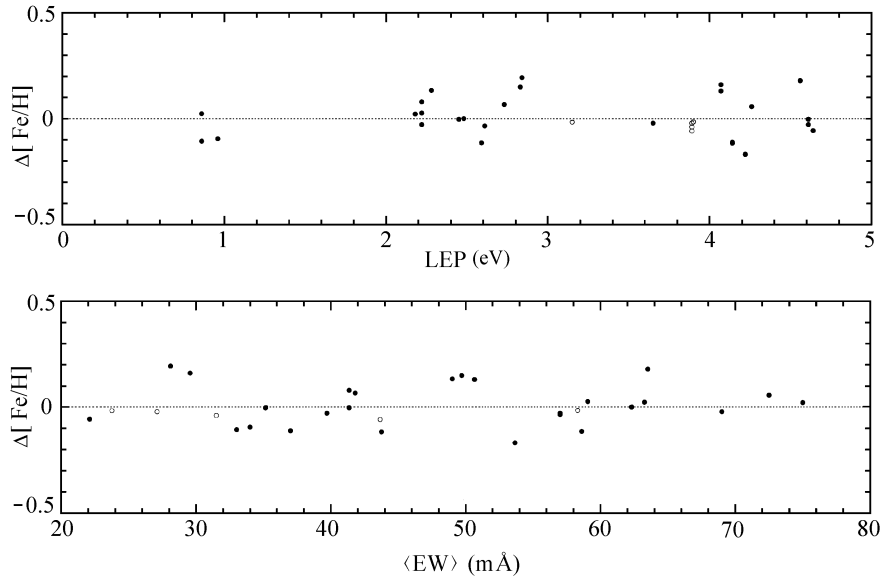


Fig. 1 Difference in iron abundance between HD 219175 A and B as a function of lower excitation potential and average equivalent width of the two components. Filled circles refer to abundances from Fe I lines, open circles, from Fe II lines.

Table 1 Stellar Parameters

Name	T_{eff} (K)	$\log g$	[Fe/H]	ξ_t	Mass (M_{\odot})
HD 219175 A	5906	4.37	-0.37	1.60	1.01
HD 219175 B	5365	4.34	-0.39	0.62	0.78

The abundance analysis was based on a net of constant-flux, homogeneous, LTE model atmospheres interpolated from the extensive grids of Kurucz (1993). With the code ABONTEST8, which is kindly provided by Pierre Magain, the abundances were derived by matching that the model calculated observed equivalent widths.

To reduce the uncertainties in the abundance determinations, we analyzed our EW data of these two stars with an approach similar to that in Laws & Gonzalez (2001). Instead of determining the chemical abundances of each star by averaging the results acquired from individual lines and subsequently comparing these averages between stars, this differential analysis method determines the differential chemical abundances between the stars by taking the differences in abundances calculated for each line individually. This approach effectively eliminates uncertainties in $\log gf$ -values and allows one to take advantage of the increased precision in $\Delta[X/H]$ for the two stars.

Table 2 lists the wavelength, LEP, $\log gf$, empirical enhancement factor (E_{γ}), EW of HD 219175 A and B, and the abundance differences between the two components for individual lines. Table 3 lists the average abundance results relative to the sun, $[X/H]_{\text{A}}$, for HD 219175 A, the average abundance differences, $\Delta[X/H]_{(\text{A}-\text{B})}$, along with rms scatter of individual values of the mean abundance and number of lines for the differential analysis.

Table 2 Line Data and EWs of HD 219175A and B

Ion	Wavelength [Å]	LEP [eV]	$\log gf$	E_γ	$EW(A)$ [mÅ]	$EW(B)$ [mÅ]	Difference [A-B]
FeI	5753.13	4.26	-0.686	1.4	69.0	76.0	0.057
	5916.26	2.45	-2.994	1.3	32.7	50.0	-0.003
	6027.06	4.07	-1.089	1.4	48.8	52.5	0.131
	6165.36	4.14	-1.473	1.4	28.0	46.0	-0.111
	6173.34	2.22	-2.880	1.2	49.0	65.0	-0.028
	6180.21	2.73	-2.586	1.4	35.0	48.6	0.067
	6200.32	2.61	-2.442	1.4	49.0	65.0	-0.034
	6229.23	2.84	-2.805	1.4	24.0	32.2	0.194
	6232.65	3.65	-1.223	1.4	63.0	75.0	-0.021
	6240.65	2.22	-3.269	1.2	34.0	48.7	0.080
	6265.14	2.18	-2.500	1.2	70.0	80.0	0.022
	6297.80	2.22	-2.733	1.2	52.6	65.5	0.027
	6322.69	2.59	-2.446	1.3	48.7	68.5	-0.114
	6358.69	0.86	-4.166	1.1	54.5	72.0	0.024
	6481.88	2.28	-2.972	1.2	44.0	54.0	0.134
	6498.94	0.96	-4.699	1.1	20.0	48.0	-0.094
	6518.37	2.83	-2.455	1.4	46.0	53.4	0.150
	6752.72	4.64	-1.280	1.4	16.5	27.7	-0.056
	6810.27	4.61	-0.986	1.4	29.6	40.7	-0.003
	6855.17	4.56	-0.614	1.4	64.0	63.0	0.180
	6858.15	4.61	-0.930	1.4	33.4	46.0	-0.028
	6978.86	2.48	-2.490	1.3	55.3	69.3	0.000
	7219.68	4.07	-1.621	1.4	27.1	32.0	0.161
7418.67	4.14	-1.445	1.4	34.5	53.0	-0.116	
7710.37	4.22	-1.112	1.4	43.0	64.3	-0.168	
7912.87	0.86	-4.848	1.1	18.0	48.0	-0.106	
FeII	5991.38	3.15	-3.557	2.5	27.0	20.5	-0.016
	6149.25	3.89	-2.724	2.5	31.5	22.7	-0.021
	6247.56	3.89	-2.329	2.5	50.0	37.3	-0.058
	6416.93	3.89	-2.740	2.5	36.5	26.5	-0.039
6456.39	3.90	-2.075	2.5	68.0	48.6	-0.015	
LiI	6707.76	0.00	0.178	1.0	42.0	-	>1.49
OI	7771.95	9.14	0.333	2.5	76.0	40.8	0.043
	7774.18	9.14	0.188	2.5	60.0	38.1	-0.119
	7775.40	9.14	-0.034	2.5	48.0	21.1	0.115
NaI	6154.23	2.10	-1.570	2.0	17.0	26.5	0.065
	6160.75	2.10	-1.228	2.0	31.0	52.4	-0.041
MgI	5711.10	4.34	-1.724	2.5	75.0	93.7	0.069
AlI	7835.32	4.02	-0.580	2.5	20.5	33.5	-0.046
	7836.13	4.02	-0.400	2.5	33.9	34.0	0.199
SiI	5772.15	5.08	-1.665	1.3	29.0	34.0	0.002
	5793.08	4.93	-1.946	1.3	26.4	35.0	-0.064
	6142.49	5.62	-1.434	1.3	21.0	19.2	0.130
	6145.02	5.62	-1.422	1.3	21.0	21.0	0.085
	7405.79	5.61	-0.681	1.3	73.0	77.5	-0.016
7415.96	5.61	-0.710	1.3	82.0	83.3	0.022	
KI	7698.98	0.00	-0.160	1.5	135.0	181.0	-0.024
CaI	6166.44	2.52	-1.189	1.8	47.5	69.0	-0.034
	6455.60	2.52	-1.350	2.0	43.0	56.0	0.103

Table 2 (Continued)

Ion	Wavelength [Å]	LEP [eV]	$\log gf$	E_γ	$EW(A)$ [mÅ]	$EW(B)$ [mÅ]	Difference [A-B]
	6471.67	2.52	-0.694	0.8	73.0	81.0	0.058
	6499.65	2.52	-0.818	0.8	60.0	80.0	-0.132
ScII	6604.60	1.36	-1.160	2.5	27.4	27.8	-0.015
TiI	5866.46	1.07	-0.805	1.5	30.0	48.0	0.130
	6258.11	1.44	-0.431	1.5	27.0	47.9	0.049
	8426.51	0.83	-1.253	1.5	22.0	59.3	-0.190
VI	6090.22	1.08	-0.062	1.5	9.0	23.2	0.058
CrI	5787.93	3.32	-0.181	2.5	22.0	37.1	0.015
	6978.38	3.46	0.142	2.5	29.0	47.6	-0.017
	7355.89	2.89	-0.285	2.5	36.0	59.0	-0.044
	7400.19	2.90	-0.166	2.5	43.6	64.0	0.005
MnI	6013.50	3.07	-0.251	2.5	44.0	65.7	-0.059
	6021.80	3.07	-0.090	2.5	58.8	74.8	0.032
Nil	6086.29	4.26	-0.530	2.5	19.0	25.2	0.066
	6108.12	1.68	-2.675	2.5	41.5	56.0	0.064
	6111.08	4.09	-0.870	2.5	25.0	27.7	0.169
	6130.14	4.26	-0.960	2.5	11.6	18.0	0.007
	6176.82	4.09	-0.260	2.5	42.0	53.0	0.024
	6327.60	1.68	-3.110	2.5	17.0	37.8	-0.080
	6767.78	1.83	-2.173	2.5	58.5	67.0	0.128
	6772.32	3.66	-0.980	2.5	37.0	53.0	-0.058
	7122.21	3.54	-0.229	2.5	76.3	85.0	0.069
	7385.24	2.74	-2.051	2.5	16.0	29.0	-0.012
	7727.62	3.68	-0.314	2.5	76.0	90.0	0.001
	7788.93	1.95	-2.075	2.5	59.5	80.0	-0.062
CuI	5782.14	1.64	-1.780	1.5	36.0	49.6	0.034
BaII	5853.69	0.60	-1.006	3.0	71.8	61.5	0.031

Table 3 Abundance Results

Element	$[X/H]_A$	$\Delta[X/H]_{(A-B)}$	rms	N	$\Delta[X/H]_{(A-B)}$ (Gratton et al.)
Fe	-0.37	0.006	0.017	31	0.00
O	-0.20	0.013	0.056	3	-0.08
Na	-0.39	0.012	0.037	2	-0.05
Mg	-0.47	0.069		1	0.03
Al	-0.48	0.077	0.087	2	-
Si	-0.29	0.026	0.026	6	0.01
K	-0.01	-0.024		1	-
Ca	-0.36	-0.001	0.045	4	0.00
Sc	-0.43	-0.015		1	-0.03
Ti	-0.38	-0.004	0.078	3	0.00
V	-0.67	0.058		1	0.10
Cr	-0.50	-0.010	0.011	4	-0.05
Mn	-0.45	-0.013	0.032	2	-0.03
Ni	-0.39	0.026	0.021	12	-0.09
Cu	-0.38	0.034		1	-
Ba	-0.14	0.031		1	-

4 DISCUSSION

We have presented the chemical abundances of HD 219175 A and B using a precise differential analysis method. The obtained lithium abundance of HD 219175 A is $\log N(\text{Li})=2.39$, while the upper limit of HD 219175 B is 0.90. The difference can be explained by depletion in the photosphere of low mass stars. In Fig.2 we plot abundance differences for the 16 observed elements other than lithium against the condensation temperature, T_c . Inspecting this figure, we find no significant difference between the abundances of the two components of HD 219175 for the 16 elements analyzed here and no clear correlation with the condensation temperature.

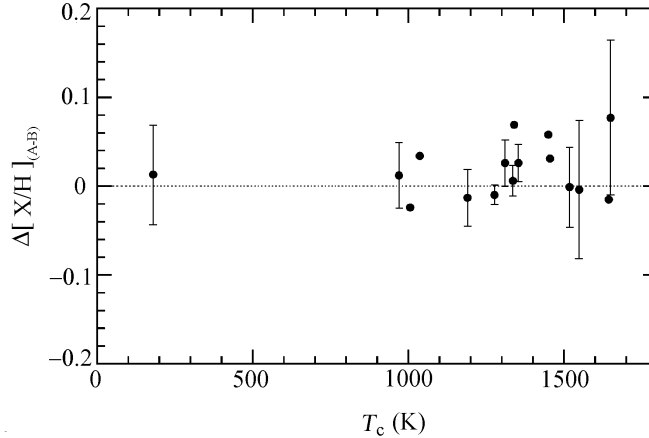


Fig.2 Run of the difference in abundances between two components as a function of the condensation temperature.

For comparison, the abundance differences from Gratton et al. (2003) are given in Table 3. Their results by standard LTE abundance analysis also showed the abundance differences of HD 219175 A and B to be small. Our abundance results support a physical relation between HD 219175 A and B. The fact that two components of HD 219175 have same chemical composition implies the binary formed in a common primordial environment and their photospheric composition (except lithium) has not changed during their evolutionary history. Some works (e.g. Gonzalez 1997) claimed pollution phenomena during evolution of stars with planets, although Desidera et al. (2004) did not find any pair among 23 binary systems with large composition differences.

Recent studies of abundance differences in binary systems mostly focused on systems with solar metallicity. Our study of a binary with lower metallicity may help understand the formation and evolution of binary systems.

Acknowledgements This research is supported by the National Natural Science Foundation of China under grant number 10433010 and NKBRFSF No. G1999075406.

References

- Alonso A., Arribas S., Martinez-Roger C., 1996, *A&A*, 313, 873
Chen Y. Q., Nissen P. E., Zhao G., Zhang H. W., Benoni T., 2000, *A&AS*, 141, 491
Desidera S., Gratton R. G., Scuderi S. et al., 2004, *A&A*, 420, 683
ESA, 1997, *The Hipparcos and Tycho Catalogues*, ESA SP-1200
Gonzalez G., 1997, *MNRAS*, 285, 403
Gratton R. G., Bonanno G., Bruno P. et al., 2001, *A&A*, 377, 123
Gratton R. G., Carretta E., Claudi R. et al., 2003, *A&A*, 404, 187
Laws C., Gonzalez G., 2001, *ApJ*, 553, 405
Nordström B., Mayor M., Andersen J. et al., 2004, *A&A*, 418, 989
Sadakane K., Ohkubo M., Honda S., 2003, *PASJ*, 55, 1005
Tokovinin A. A., Smekhov M. G., 2002, *A&A*, 382, 118
VandenBerg D. A., Swenson F. J., Rogers F. J. et al., 2000, *ApJ*, 532, 430
Zhang H. W., Zhao G., 2004, *A&A*, submitted
Zhao G., Li H. B., 2001, *Chin. J. Astron. Astrophys.*, 1, 555